JACS
JOURNAL OF THE AMERICAN CHEMICAL SOCIETY

Article

pubs.acs.org/JACS

Remote-Stereocontrol in Dienamine Catalysis: *Z*-Dienamine Preferences and Electrophile–Catalyst Interaction Revealed by NMR and Computational Studies

Andreas Seegerer,[†] Johnny Hioe,[†] Michael M. Hammer,[†] Fabio Morana,[†] Patrick J. W. Fuchs,[‡] and Ruth M. Gschwind*[,†]

[†]Institut für Organische Chemie, Universität Regensburg, D-93053 Regensburg, Germany

[‡]Institut für Organische Chemie, Universität Leipzig, D-04103 Leipzig, Germany

Supporting Information

ABSTRACT: Catalysis with remote-stereocontrol provides special challenges in design and comprehension. One famous example is the dienamine catalysis, for which high ee values are reported despite insufficient shielding of the second double bond. Especially for dienamines with variable *Z*/*E*-ratios of the second double bond, no correlations to the ee values are found. Therefore, the structures, thermodynamics, and kinetics of dienamine intermediates in S_N-type reactions are investigated. The NMR studies show that the preferred dienamine conformation provides an effective shielding if large electrophiles are used. Calculations at SCS-MP2/CBS-level of theory and experimental data of the dienamine formation show kinetic preference for the *Z*-isomer of the second double bond and a slow isomerization toward the thermodynamically preferred *E*-isomer. Modulations of the rate-determining step, by variation of the concentration of the electrophile, allow the conversion of dienamines to be observed. With electrophiles, a faster reaction of *Z*- than of *E*-isomers is observed experimentally. Calculations corroborate these results by correlating ee values of three catalysts with the kinetics of the electrophilic attack and reveal the significance of CH–π and stacking interactions in the transition states. Thus, for the first time a comprehensive understanding of the remote stereocontrol in γ-functionalization reactions of dienamines and an explanation to the "*Z*/*E*-dilemma" are presented. The combination of bulky catalyst subsystems and large electrophiles provides a shielding of one face and causes different reactivities of *E*/*Z*-dienamines in nucleophilic attacks from the other face. Kinetic preferences for the formation of *Z*-dienamines and their unfavorable thermodynamics support high ee values.

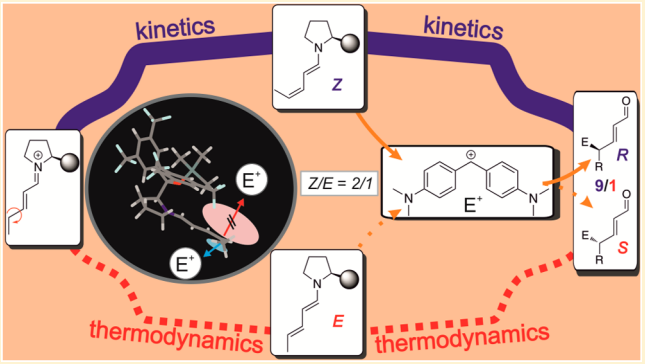

INTRODUCTION

Remote-stereocontrol is a noble goal in asymmetric catalysis but a challenge in understanding and design. Prominent examples for the application of this remote-stereocontrol in organocatalysis are found in dienamine,[1−3] trienamine,[3,4] and tetraenamine[3,5] transformations. In some of these reactions, very high ee values were reported, and for the sterically demanding Diels–Alder-type reactions, a plausible reaction mechanism was proposed.[2,6] However, for S_N-type γ-functionalization of dienamines detailed mechanistic studies and experimental insights into the underlying mechanism are, to our knowledge, very limited. This may obviously hamper the further development of the field. The main points under question are the partial shielding of the catalyst moiety and the "*Z*/*E*-dilemma" of the second double bond in linear aldehydes (see Figure 1) similar to the "*Z*/*E*-dilemma" known for iminium ion catalysis.[7]

The dienamine catalysis, which is closely related to the enamine catalysis, has emerged as one of the most promising

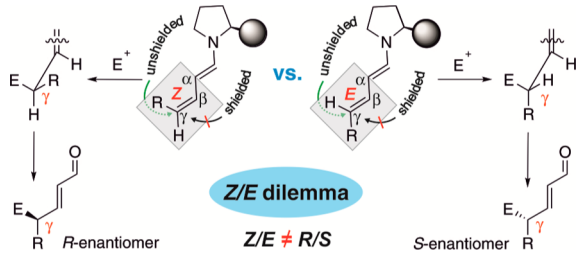

Figure 1. "*Z*/*E*-dilemma" in dienamine catalysis, i.e., the correlation between the *Z*/*E*-ratio of the second double bond and the *R*/*S*-ratio of the products is in dispute.

stereoinducing catalytic models in the α- and γ-functionalization of unsaturated aldehydes.[1,2,8−13] This concept represents a vinylogous version of enamine activation, magnifies the

Received: April 19, 2016
Published: July 19, 2016

DOI: 10.1021/jacs.6b04008
J. Am. Chem. Soc. 2016, 138, 9864−9873

nucleophilic character of the γ-carbon, and enables functionalization reactions of conjugated aldehydes at their α- or γ-position (Figure 2).[2] The first selective γ-functionalization of

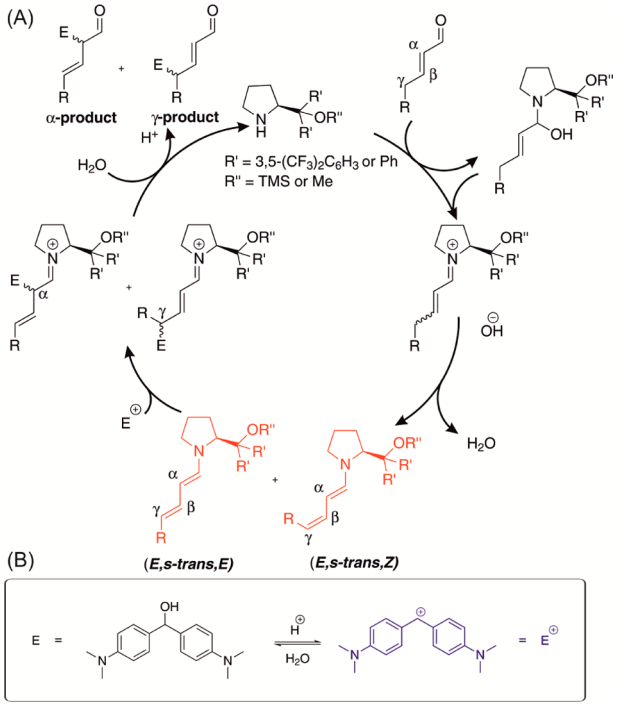

Figure 2. S_N-type dienamine reaction. (A) Proposed catalytic cycle based on previous publications.[2,11,12] (B) Acid-catalyzed equilibrium between the electrophile source E = bis(4-dimethylaminophenyl) methanol (Michler's hydrol) and the corresponding electrophile E^+.[34,35]

unsaturated aldehydes with Jørgensen–Hayashi-type catalysts[3,14−16] was presented by Jørgensen et al. in 2006.[2] Later, the principle of γ-functionalization of dienamines was extended to S_N1-type reactions with bis[4-(dimethylamino)phenyl]-methanol as electrophile source by Christmann et al. in 2011.[12] In their study, mixtures of α- and γ-alkylated products were obtained. For aldehydes, which are disubstituted at the γ-position, the α-alkylated aldehyde was observed as a major product, and in the case of monosubstituted aldehydes, the γ:α ratio is inverse. For the γ-alkylation, high to moderate enantioselectivities were achieved (the longer the chain length of the aldehyde, the lower the ee values). Later in 2012, Melchiorre et al.[11] managed to circumvent these synthetic limitations associated with the geometry control and site selectivity by using α-substituted unsaturated aldehydes. Hence, the formation of α-product is completely suppressed in this case.

In the field of secondary aminocatalysis, especially in the fields of enamine[17−26] and iminium ion activation,[7,27−31] recently some mechanistic insights could be gained in terms of intermediate stabilization, stereoselection modes, and reaction mechanisms. In the first dienamine study[2] already structural properties of the diene system (*E,s-trans,E* and *E,s-trans,Z*, including a *Z*/*E*-ratio for the second double bond of 2/1) were solved by NMR. For α-substituted dienamines, Melchiorre et al. characterized the diene system using NMR analysis and theoretical calculations.[11] In contrast to linear dienamines (*Z*/*E* = 2/1), α-substituted ones showed exclusively an *E* configuration of the second double bond and both isomers (*E* and *Z*) of the first double bond. This inverted structural preference of the second double bond resulted also in an inversion of the stereocenter at the γ-position of the major product. However, neither in cycloadditions nor in S_N-type reactions, the *Z*/*E*-ratios fit to the experimental ee values, if a classical shielding model is assumed. Therefore, it became even more pressing to rationalize the correlation between the *Z*/*E*-ratio of the second double bond and the stereochemical outcome.

A potential explanation to this phenomenon is the different stabilization of the transition states toward the two downstream iminium ion intermediates. Indeed, computational studies revealed a kinetically controlled [4+2] Diels–Alder reaction pathway with interactions in the product iminium ion transition state controlling the stereochemical outcome of the reaction.[2,6] In the case of diethyl azodicarboxylate (DEAD) as electrophile, a downstream isomerization of the double bond in the product was proposed to be responsible for the synthetically observed γ-functionalized unsaturated aldehydes.[2,32] For other [4+2] cycloadditions of dienamines, the higher stabilization of the zwitterionic *endo*-iminium intermediate and the corresponding reaction pathway was identified to be responsible for the high stereoselectivity.[6] Furthermore, a computational study of a [5+2] cycloaddition using squaramide-derived bifunctional organocatalysts (providing a preorganization of the electrophile by hydrogen bonds) corroborated the importance of configurational preferences and π–π interactions within the transition states for the diastereomeric ratio.[33] However, for S_N-type reactions of dienamines, it is still unclear how the stereoselectivity is connected to the *Z*/*E*-ratio. Furthermore, *in situ* reaction monitoring of dienamine reactions revealing potential time dependences of the *Z*/*E*-ratios or a faster reaction of *E*- or *Z*-dienamine with electrophiles has not been performed so far.

Therefore, here we present a detailed NMR study of all structural features of dienamines (including the conformation of the catalyst subsystem) validating our computational studies of the dienamine ground states. In addition, theoretical studies of the dienamine reaction pathway were underpinned and compared with experimental kinetic studies of the formation and conversion of various dienamines, which were enabled by intentional shifts of the rate-determining step. With these methods, we gained detailed insights into the stereoselection mode of S_N-type dienamine reactions and could explain the "*Z*/*E*-dilemma".

RESULTS AND DISCUSSION

Model System and Theoretical Levels. To investigate the structural preferences, intermediates, and stereoselection modes in S_N-type dienamine reactions, we selected as a model reaction the γ-alkylation of α,β-unsaturated aldehydes with bis(4-dimethylamino-phenyl)methanol **E** (Figure 2B). As catalysts Jørgensen–Hayashi prolinolethers[15,16,36] **A**–**C** (Figure 3B) were chosen, since they are known in dienamine catalysis to result in high ee values and good yields.[1,2,11,12] In addition, we were experienced in the structural elucidation of intermediates using these catalysts from our enamine studies.[22−26] To reduce the amount of α-substituted product,[12] γ-methyl substituted (4-methyl-2-pentenal **4**) and linear α,β-unsaturated aldehydes ((*E*)-2-pentenal **1**, (*E*)-2-heptenal **2**, (*E*)-2-decenal **3**) with different chain lengths were selected. This leads to a modulation of steric and electronic properties. α-Substituted aldehydes were omitted due to their exclusive *E*-configuration of the second double bond. Therefore, they do

DOI: 10.1021/jacs.6b04008
J. Am. Chem. Soc. 2016, 138, 9864−9873

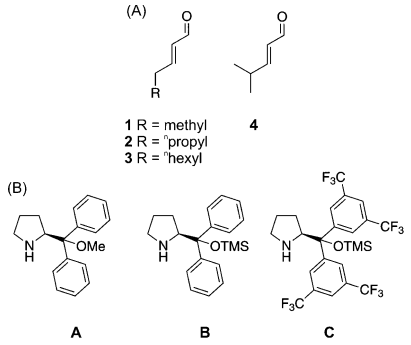

Figure 3. Model systems for structural studies and reaction monitoring. (A) aldehydes **1**−**4**; (B) Jørgensen−Hayashi type catalysts **A**−**C**.

not allow an insight into the correlation between *Z*/*E*-isomerization of the second double bond and its influence on the stereoselectivity.[11] Bis(4-dimethylaminophenyl)-methanol **E** (Figure 2B), also known as Michler's hydrol, was chosen as electrophile source. It is known to form stabilized carbocations $\mathbf{E}^+$ under acidic conditions (Figure 2B).[34,35] By varying the acidity of the additive, the amount of active electrophile $\mathbf{E}^+$ can be controlled (for UV−vis spectra see Supporting Information). In addition, a Diels−Alder pathway is excluded, since the carbocationic species (E^+ see Figure 2B) reacts as an electrophile with nucleophilic reagents such as dienamines.[11,12,35] As the solvent, toluene was chosen, because it is the preferred solvent in synthesis for this reaction type.[2,11,12] In this NMR study exclusively dienamines (***E*/*Z*-1A**−**C**, ***E*/*Z*-2C**, ***E*/*Z*-3C**, **4C**) (*E* and *Z* indicates the configuration of the second double bond, see the Structure of Dienamines section) were detected as intermediates. The iminium ion or aminol species proposed in the catalytic cycle (see Figure 2A) were below the detection limit. High-level quantum chemical calculations (SCS-MP2/CBS; see computational details and Supporting Information) on dienamines were conducted and compared to the experimental data. In addition, the potential influence of iminium ion species on the reactivity and selectivity was investigated by theoretical calculations.

Structure of Dienamines. First, the formation and structures of the dienamine species were investigated by NMR analysis with samples of 1 equiv of catalyst and 1 equiv of aldehyde in toluene-d_8 at 180−300 K (Figure 3).

During our investigations, we were able to detect dienamines ***E*/*Z*-1A**−**C**, ***E*/*Z*-2C**, ***E*/*Z*-3C**, and **4C**. The following structural analysis was performed for every dienamine. Generally, all dienamines show the same structural pattern regarding *E*/*Z*-configuration and conformation of the catalyst subsystem. Therefore, for the sake of clarity in the following discussion, only *trans*-2-pentenal **1** with catalyst **C** is described in detail (for other structural analysis see Supporting Information). For the description of the structural motif of these isomers, first the diene subsystem is discussed and then the structure of the catalyst subsystem.

In the diene subsystem (Figure 4), the first N−C1 single bond can principally adopt two conformations (*s-trans*, *s-cis*). However, similar to the structural preferences of enamines with catalysts **A**−**C**,[23] exclusively the *s-trans* conformation is identified in solution for dienamines. This can be confirmed by strong NOE signals between H_1 and H_α, weak interactions between H_1 and $H_{\delta1,2}$ as well as large $^3J_{CH}$ couplings between H_1 and C_δ (see Supporting Information). The structural

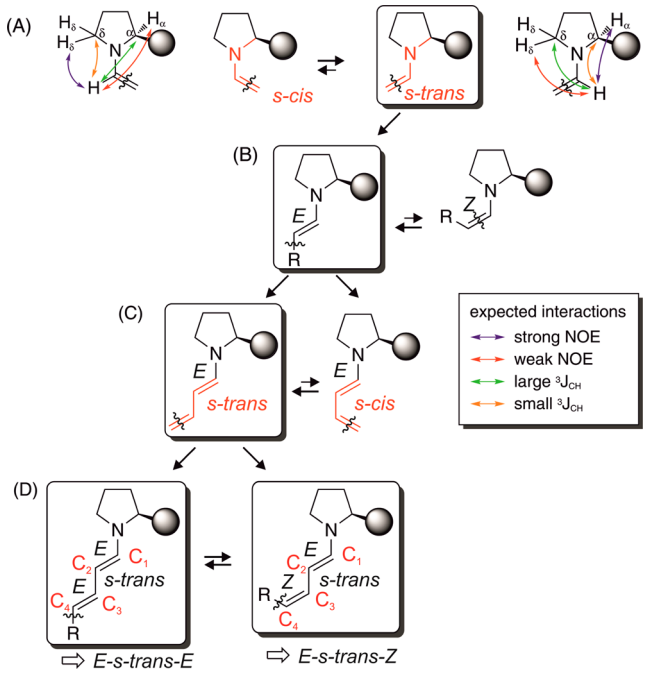

Figure 4. Structural preferences of the diene subsystem. The conformations/configurations detected by NMR and the corresponding nomenclature are highlighted by boxes. For details, see text.

preferences of the C_1-C_2 double bond and the C_2-C_3 single bond were determined by $^3J_{HH}$ coupling constant analysis. For the C_1-C_2 double bond, $^3J_{HH}$ coupling constants of 13.2−13.5 Hz were found. In agreement with previous NMR studies,[11] theoretical calculations,[2] and our studies of enamines,[22−25] this indicates *E* configured C_1-C_2 double bonds for all dienamine systems under investigation (for $^3J_{HH}$ see Supporting Information). The C_2-C_3 single bond showed smaller $^3J_{HH}$ couplings in the range of 10.3−11.3 Hz (see Supporting Information). These values are in good agreement with other literature known examples for *s-trans* diene systems (10.4−11.2 Hz).[37−39] The first variability within the diene system of the two isomers is related to the configuration of the second double bond between C_3 and C_4 (Figure 4D). Dependent on the length of the alkyl moiety attached to the diene system and on the catalyst applied, *Z*/*E* ratios between 0.88 and 2.16 were detected (***Z*/*E*-1A** = 1.9/1; ***Z*/*E*-1B** = 2/1; ***Z*/*E*-1C** = 2.16/1; ***Z*/*E*-2C** = 1.04/1; ***Z*/*E*-3C**= 0.88/1; for details see Supporting Information).

Next, we investigated the structural and conformational preferences of the catalyst moiety. The exocyclic bond of the catalyst can adopt three conformations, namely *sc-endo*, *sc-exo*, and *ap* (see Figure 5B).[23] Using similar structural NMR investigations as previously applied for enamine intermediates with catalysts **A**−**C**,[23,40] we found the same *down*-puckering of the pyrrolidine ring indicated by an $H_{\gamma2}$ highfield shift in dienamines in comparison to the free catalyst (see Figure 5A; $\Delta\delta$ ($H_{\gamma2}$) = −0.54 to −0.79 ppm; for details see Supporting Information). This shift is caused by CH−π interactions of the aromatic moieties of the catalyst and $H_{\gamma2}$ in the *sc-exo* or *ap* arrangement. Quantum chemical calculations of the Boltzmann averaged dienamine structures corroborate these experimental data. The Gibbs free energy of *sc-endo* is about 33 kJ/mol above the global minimum at SCS-MP2/CBS level of theory and therefore thermally not populated at our reaction conditions. The NOESY spectra of all investigated dienamine systems

DOI: 10.1021/jacs.6b04008
J. Am. Chem. Soc. 2016, 138, 9864−9873

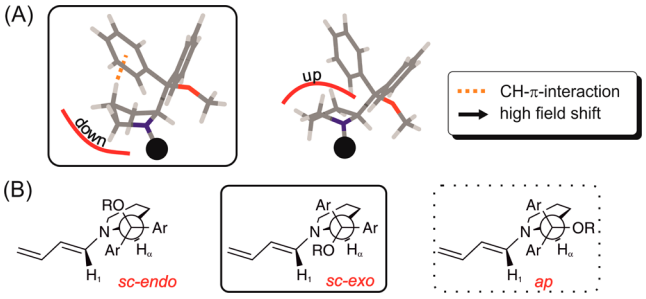

Figure 5. Structural preferences of the catalyst subsystem. The boxes highlight the experimentally found preferences for the puckering of the proline ring as well as for the exocyclic bound moiety of the catalyst. The dashed box indicates a population of *ap* conformer predicted by theoretical calculations.

showed interactions between H_1 and the protons of the O-protecting group, which is only plausible in the *sc-exo* conformation. Theoretical distance calculations for ***E*/*Z*-1C** showed a NOE-averaged distance of H_1 to H_{OTMS} of 6.00 Å for *ap* and 3.47 Å for *sc-exo*. Using NOESY measurements, the experimental averaged distance between these nuclei was calculated to be 3.80 Å (see Supporting Information for the equation). The detection of this key NOE proves positively the existence of the *sc-exo* conformation. The larger distance is a potential hint for the coexistence of *ap*-conformers, however the experimental error of the NOE in our case does not allow for reliable quantification. The related theoretical calculations predicted almost the same energy for *sc-exo* and *ap* (ΔG_{exoap} = −0.9 kJ/mol for ***E*-1C**), which is a second indication for the presence of the *ap* conformation in solution.

Subsequently, the shielding of the diene subsystem was investigated by theoretical structure calculations including the experimentally determined preferences discussed above. The calculated 3D models (Figure 6) showed a shielded face of the first double bond within the diene systems (α-position), which hinders an attack of an electrophile comparable to the shielding of the α-position in enamine catalysis.[14] The second double bond (γ-position) is only partially shielded, leading to the problem of remote stereocontrol in dienamines. This partial shielding makes it highly probable that the size of the electrophile influences the effectiveness of the catalyst shielding. Thus, for small electrophiles, only poor stereoselectivities are expected. For bulky electrophiles, the partial shielding should be much more effective. Indeed, in dienamine reactions with Michler's hydrol derivatives as electrophiles (bulky electrophiles), high ee values were reported for α-substituted enals[11] and our model system *trans*-2-pentenal **1**,[12] whereas to our knowledge, for very small electrophiles, high stereoselectivities have not been reported so far. This structural analysis is in agreement with our theoretical calculations of an electrophilic attack from the shielded face in γ-position. The calculated energy barriers (approximately 80 kJ/mol) for an attack in γ-position of both dienamines (***E*-** and **Z-1C**) on the carbocationic species $\mathbf{E}^+$ is substantially higher than those of the attack from the unshielded face (44−49 kJ/mol). That means for large electrophiles such as Michler's hydrol, the partially shielded face of dienamine structures is kinetically not accessible even in the γ-position (Figure 6).

One consequence of these combined experimental and theoretical investigations is that the reported ee value in dienamine catalysis with Michler's hydrol has to originate from a stereodiscrimination between the attack either on *E*-

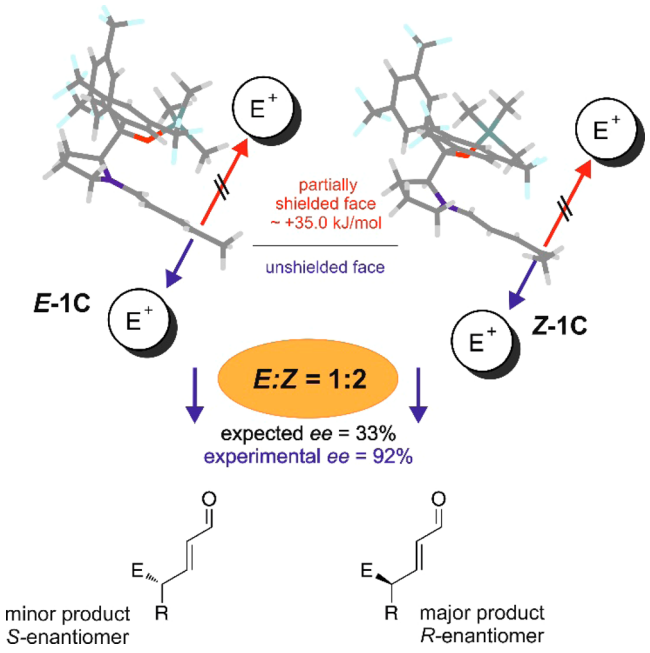

Figure 6. Shielding and remote stereocontrol in dienamines. Top: 3D models of dienamine ***E*/*Z*-1C** show a partially shielded face from the top side. For bulky electrophiles, this partial shielding is sufficient to block electrophilic attacks even in the γ-position (~35 kJ/mol higher energy barriers). Bottom: kinetically preferred attack of both isomers from the unshielded face yielding different enantiomers. Black: expected ee value, if both isomers (*E*/*Z* = 1/2) react with the same rate. Blue: experimental ee values.

dienamine or *Z*-dienamine from the unshielded face. For our catalyst **C** with *trans*-2-pentenal **1**, a *Z*/*E*-ratio of 2/1 was found experimentally. This distribution of isomers was already observed before by Jørgensen et al.[2] In the case, both *E*- and *Z*-dienamines would react with the electrophile via an isoenergetic barrier, and this *Z*/*E*-ratio of 2/1 would result in an ee value of 33%. However, as shown in our work and also in literature, ee values of around 92% are obtained for this reaction (Figure 6).[12] In principle, this deviation between structure related and experimental ee values can have two possible causes; first, the experimentally observed *Z*/*E*-ratio deviates drastically from that active in the catalysis (kinetic versus thermodynamic control), or second, the activation barriers from *E*-dienamine and *Z*-dienamine deviate significantly in their downstream reactions. Of course, combinations of both reasons are also highly probable.

Enantioselectivity and Kinetic Control. To examine the origin of the so far unexplained stereoselection mode of the electrophilic attack in γ-position of dienamines from the unshielded face including also the *Z*/*E*-ratio, we investigated the kinetics and thermodynamics of dienamine formation and the conversion with Michler's hydrol by NMR and theoretical calculations.[41] First, the formation rates of *Z*-dienamines versus *E*-dienamines were addressed. Under experimental conditions typically used in synthesis, the formation of dienamines is the rate-determining step, followed by a fast addition of the electrophile (see discussion below). In these setups, dienamines cannot be detected by NMR. Therefore, our structural investigations of the dienamines were previously performed exclusively without electrophile. A kinetically controlled, extremely high *Z*/*E*-ratio (about 24/1 for an ee value of 92%) combined with a subsequent fast isomerization toward

DOI: 10.1021/jacs.6b04008
J. Am. Chem. Soc. 2016, 138, 9864−9873

the thermodynamic ratio of *Z*/*E* could therefore easily explain the deviation between the ee values obtained in synthesis and the *Z*/*E*-ratio observed in NMR studies.

The NMR determined *Z*/*E*-ratio of the double bond between C_3 and C_4 in all investigated dienamines showed an uncommon high amount of *Z*-isomer (up to a *Z*/*E*-ratio of 2.16:1 for ***E*/*Z*-1C**; for the time of determination see Supporting Information). This deviates clearly from previous[2] and our current theoretical calculations of the relative dienamine ground-state energies (here with *trans*-2-pentenal **1** as aldehyde), which suggested that the *E*-isomer is marginally more stable than the *Z*-isomer by 0.6 kJ/mol for catalyst **B** to 2.9 kJ/mol for catalyst **C**. The latter (dienamine ***E*/*Z*-1C**) corresponds to a thermodynamic *Z*/*E*-ratio of 24:76 (see Figure 7A). This is in good agreement with the work of Jørgensen et al. at a lower level of theory (B3LYP/6-31G(d))[2] and indicates a kinetic preference for *Z*-dienamines. Our current calculations showed that the transition state for the deprotonation of iminium ion precursors with a base catalyst model ((*S*)-2-(methoxymethyl)pyrrolidine) leading to *Z*-dienamine is lower by 3 kJ/mol than to *E*-dienamine. A close inspection of the transition-state structures reveals higher steric hindrance in case of the *E*-dienamine as the most probable reason for this energy difference. The lower barrier for the formation of *Z*-dienamine is also predicted when NMe_3 is used as deprotonating agent, which would indicate that the choice of the base is rather insignificant. According to Eyring theory, this energy difference in barrier heights corresponds to a 3.3-fold faster formation of *Z*-dienamine compared to *E*-dienamine, which is similar to the observed ratio of 2/1 for *Z*/*E* (Figure 7A).

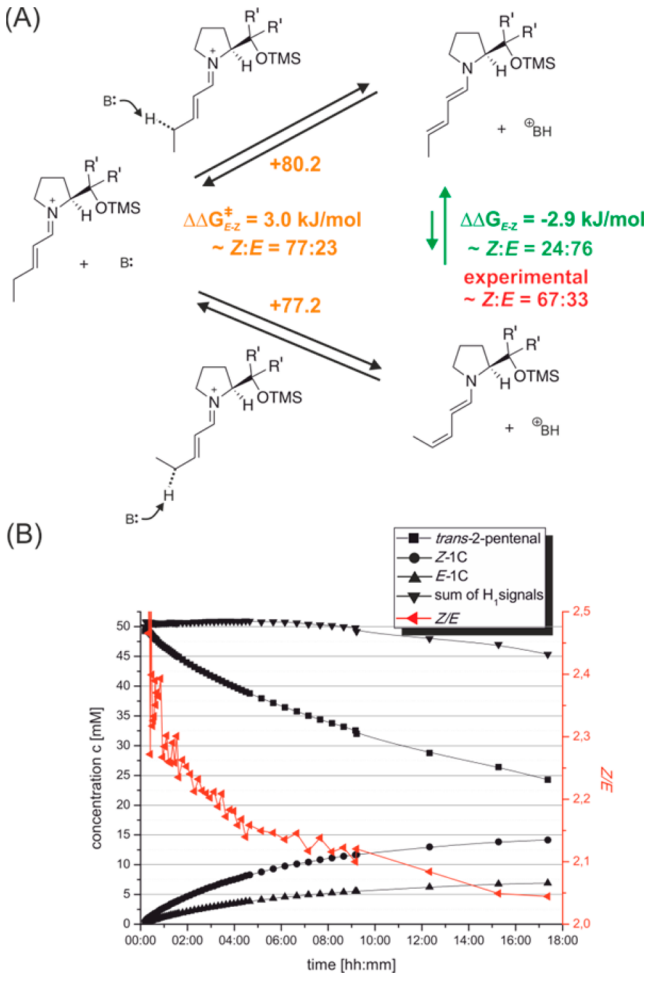

Figure 7. Kinetic control of the *Z*/*E*-ratio of dienamines. (A) Theoretically predicted barriers of dienamine formation from iminium ion precursors agree very well with the experimental values, whereas the thermodynamic distribution of the dienamine ***E*/*Z*-1C** is inverse. All energies are depicted in kJ/mol. (B) NMR reaction profiles of dienamine formation of ***E*/*Z*-1C** revealing a slow but significant change of the *Z*/*E*-ratio support the kinetic preference for *Z* followed by a slow isomerization to *E* (**1** (1 equiv) and **C** (1 equiv) without acid at 300 K in toluene-d_8).

To prove experimentally that the *Z*/*E*-ratio is kinetically driven and that the *E*-isomer is the thermodynamic product, we investigated the isomerization of the second double bond toward the thermodynamic equilibrium. For this purpose ^{1}H kinetic NMR measurements of the reaction of *trans*-2-pentenal (aldehyde **1**) and catalyst **C** at different temperatures and under the influence of acid were carried out. At 300 K and without acidic additive (Figure 7B), the dienamine formation for ***E*/*Z*-1C** showed a decrease of *Z*/*E*-ratio with time (for identical measurements at higher temperatures and/or with acid, accelerated both isomerization and polymerization; see Supporting Information). The final thermodynamic equilibrium was not reached, due to emerging polymerization after around 9 h, visible on the decay of the sum of signal intensities in Figure 7B. Nevertheless, the slow but significant change of the *Z*/*E*-ratio toward higher amounts of *E* during the initial part of the reaction is in close agreement with the theoretical predictions. The very slow isomerization process lasting for hours in combination with an observed *Z*/*E*-ratio higher than the theoretically predicted one corroborates a significant kinetic preference of *Z* followed by the isomerization toward *E*, the thermodynamic preference. In addition, both experiment and calculations exclude extremely high amounts of *Z*-dienamines during the dienamine formation. Thus, an additional factor has to contribute to reach the high ee values observed in synthesis.

Therefore, the downstream reactions of the dienamines were investigated next, and further experimental and theoretical investigations of the conversion of the dienamines with the electrophile were performed. The energy barriers (black and red lines) for the conversion to the γ-product (49.6/44.0 kJ/mol) were significantly smaller than for the dienamine (***E*/*Z*-1C**) formation (80.2/77.2 kJ/mol) (Figure 8A). The calculated energy barrier difference translates to several orders of magnitude in reaction rates, which means the dienamine species is not detectable in solution in the presence of a sufficient amount of electrophile (Figure 8B; using TFA). In an S_N1 reaction (first order by nature), the rate-determining step (RDS) is generally the generation of the carbocation, and therefore its concentration is significantly lower than the nucleophile. As soon as the amount of electrophile equals/exceeds the amount of nucleophile (dienamines), the reaction is dependent on the concentration of both reactants. In the presence of strong acids, the hydrolysis of the hydrol is accelerated, the thermodynamic equilibrium is shifted providing higher concentration of E^+, and the reaction becomes second order. Thus, the reaction cannot be assigned as a classical "S_N1", and the dienamine formation seems to be the RDS. Due to the very fast conversion of dienamines, it is not possible to investigate deviating reaction rates of *Z*- and *E*-dienamines experimentally. Therefore, it was crucial for further experiments to reduce significantly the rate of the electrophilic attack by

DOI: 10.1021/jacs.6b04008
J. Am. Chem. Soc. 2016, 138, 9864−9873

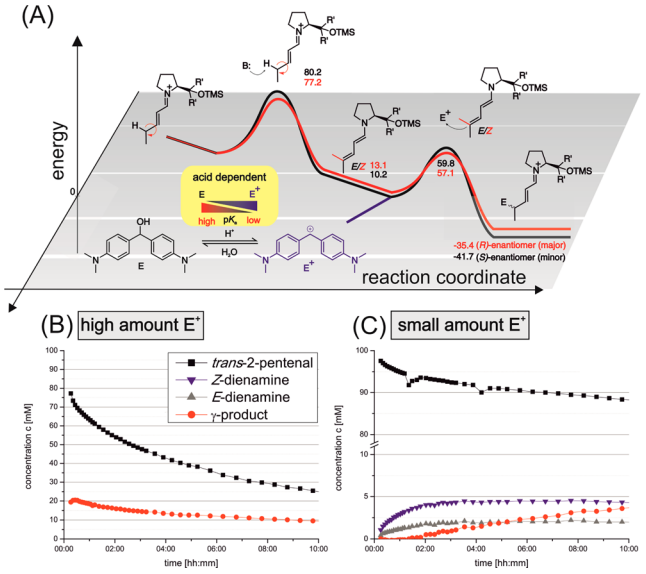

Figure 8. Energy profiles of dienamine reactions and modulation of the RDS by variation of the electrophile concentration. (A) Calculated free energy surfaces ($\Delta G298$) (black ***E*-1C** and red **Z-1C** line) at SCS-MP2/CBS level of theory and schematic acid-dependent generation of carbocation E^+. (B and C) The NMR reaction profiles show the shift of the RDS; with TFA, no dienamines are detected (B), whereas with acetic acid, both dienamines are observable (C) (aldehyde **1** (2 equiv), catalyst **C** (0.2 equiv), Michler's hydrol (1 equiv), and TFA or acetic acid (0.1 equiv) at 313 K in toluene-d_8.

lowering the concentration of E^+. This has the consequence that now the nucleophile (dienamine) concentration is significantly higher than the electrophile concentration, and the rate-determining step is exclusively the generation of the electrophile (classical S_N1). The pK_a dependency of the generation of the electrophile is schematically represented in Figure 8A by the chemical equilibrium. The amount of active electrophile is varied by using the different acids (see Supporting Information for UV−vis spectra). Depending on the acid, the reaction order can be modulated, which leads to a shift of the RDS to the carbocation formation step. This is proven by the simultaneous detection of dienamines and products by NMR (Figure 8C; using AcOH).

An experimental setup with weak acid (AcOH) now allows for the investigation of the relative reactivity of *E*- and *Z*-dienamines with electrophile. In addition to the *Z*/*E*-ratio, the difference in reactivity toward electrophile is proposed as a second factor, which affects the observed ee values.

In the case of a kinetically controlled preference of the *Z*-isomer in the electrophilic attack, its amount has to decrease faster than *E*. However, in Figure 8C, both dienamines remain constant after reaching a maximum (4 h). The profile can be explained by the consumption of the free catalyst, which reduced the rate of the dienamines formation. After 4 h the rates of dienamines formation and conversion are comparable leading to a steady state. To prove the kinetic preference of *Z*-dienamines toward electrophile experimentally, kinetic measurements with higher amount of catalyst (1 equiv) and acetic acid (1 equiv) were performed (Figure 9). The adapted stoichiometric ratio provides two advantages. First, it increases the amount of the dienamines and simplifies the detection. Second and more importantly, both formation and conversion of dienamines are accelerated. After a short offset (4 h), the conversion to the γ-product is faster than the dienamine

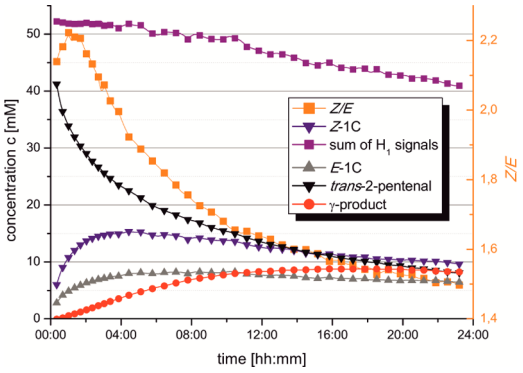

Figure 9. Reaction profile of dienamines *E*/*Z*-**1C**, the resulting *Z*/*E*-ratio, and simultaneous γ-product formation, showing a faster consumption of *Z*-dienamine. Aldehyde **1** (1 equiv), catalyst **C** (1 equiv), Michler's hydrol (1 equiv), and AcOH (1 equiv) at 313 K in toluene-d_8.

formation due to the higher concentration of electrophile E^+, which is indicated by the decrease of both dienamines. Despite the faster formation of *Z*-dienamine than *E*-dienamine, the faster conversion of *Z*-dienamine is now observable.[42] This reveals a combination of preferred formation and conversion of *Z*-dienamines as origin of the ee values observed in synthesis.

From these experimental data, the reason for the preferred electrophilic attack on *Z*- compared to *E*-dienamines is unclear. Therefore, further theoretical calculations of the electrophilic attack were conducted. For large electrophiles, the electrophilic attack from the partially shielded face is by far too high in energy (see Figure 6). Considering an exclusive attack from the unshielded side, the *E*-dienamine yields the *S*-enantiomer of the γ-substituted α,β-unsaturated product, whereas the *Z*-dienamine gives the *R*-enantiomer, which is the major product. As we have already shown, the higher population of *Z*-dienamine (~66%) cannot be solely responsible for the variation of the ee values, otherwise similar ee values across all investigated systems are expected (Table 1). Moreover, the NMR kinetic

Table 1. Calculated $\Delta\Delta G^{\ddagger}$ Values [kJ/mol] (Boltzmann averaged) for Dienamine Electrophile Adduct Formation Step for *E*/*Z*-1A−C Translated to Reaction Rate Ratios According to the Eyring Equation and the Resulting Theoretical ee Values[a]

catalyst	*Z*/*E*-ratio (approx.)	$\Delta\Delta G^{\ddagger}$ [kJ/mol]	theor reaction rate ratio *Z* vs *E*	theor ee	exptl ee
A	2/1	1.89	2.1/1	36%	27%
B	2/1	3.13	3.5/2	56%	48%
C	2/1	5.60	9.5/1	80%	78%

[a]Experimental ee values derived from reaction of aldehyde **1** (2 equiv), catalyst **A**−**C** (0.2 equiv), Michler's hydrol (1 equiv), and acetic acid (0.1 equiv) at 313 K in toluene-d_8 after 24 h.

data shown in Figure 9 indicate a kinetically controlled product conversion preferably from *Z*-dienamine. Indeed, our current predictions showed that the transition state for the electrophile attack on the open face of ***E*-1A−C** is higher than on **Z-1A−C** (Boltzmann averaged 1.90−5.60 kJ/mol; for values of ***E*/*Z*-1C** see Figure 8A).[43]

The theoretical calculations showed that the differences in the free energy barriers ($\Delta\Delta G^{\ddagger}$) between *Z* and *E* are the results of two effects: the higher thermodynamic stability of *E* compared to *Z* and the differences in dienamine−electrophile

DOI: 10.1021/jacs.6b04008
J. Am. Chem. Soc. 2016, 138, 9864−9873

interactions in the transition states. Taken together, the calculations of the transition states corroborate the faster formation of the major product from *Z*-dienamine as shown experimentally.

To confirm the kinetic control of the stereoinduction, we determined the ee values of *trans*-2-pentenal **1** with Michler's hydrol using three different catalysts (**1** (2 equiv); **A**−**C** (0.2 equiv); Michler's hydrol (1 equiv); AcOH (0.1 equiv); 313 K in toluene). Despite similar ***Z***/***E*-1A**−**C** ratios of the dienamines, the ee values between the catalysts vary strongly, with catalyst **C** being the most enantioselective and **A** the least (Table 1). If the kinetic control is valid, then the free energy differences of the transition states for the iminium ion-electrophile adduct formation will correlate with the ee values. As shown in Table 1, the highest $\Delta\Delta G^{\ddagger}$ for ***E*/*Z*-1C** (5.6 kJ/mol) reflects the highest theoretical ee value (80%), while the lowest $\Delta\Delta G^{\ddagger}$ for ***E*/*Z*-1A** (1.90 kJ/mol) reflects the lowest ee value (36%). This means that these values are in very good agreement with the experimental ee values for the different catalysts.

Next, the kinetic and thermodynamic terms in the product formation step were decomposed to track the origin of the different energy barriers. As previously described, the ***E*-1A**−**C**-dienamines are thermodynamically slightly more stable than the ***Z*-1A**−**C** dienamines ($\Delta G_{Z\text{-}E}$(**B**) = 0.6 kJ/mol; $\Delta G_{Z\text{-}E}$(**A**) = 2.5 kJ/mol; $\Delta G_{Z\text{-}E}$(**C**) = 2.9 kJ/mol). Excluding the thermodynamics, the highest pure kinetic effect from the transition states is calculated for catalyst **C** ($\Delta\Delta G^{\ddagger} - \Delta G_{Z\text{-}E}$ = 5.60 − 2.9 = 2.7 kJ/mol), while the lowest is estimated for catalyst **A** ($\Delta\Delta G^{\ddagger} - \Delta G_{Z\text{-}E}$ = 1.9 − 2.5 = −0.6 kJ/mol). The positive value for **C** means that the transition state between *E*-dienamine and the electrophile is more unstable than the *Z*-dienamine and vice versa for **A**. At first glance, the altering stability of the transition states is very puzzling, because both transition states possess the same conformational preference, (*ap*-conformation and *down*-puckering). Hence a precise structure analysis was performed.

From the structure analysis of the transition states, several distinctive interactions could be identified: (1) stabilizing CH−π interactions between C_5 bound protons of the diene system (e.g., methyl group in ***E*/*Z*-1A**−**C**) and one of the aromatic rings of the electrophile (Figure 10A highlighted in yellow), which are present in all transition states of *Z*-dienamines but not in *E*-dienamines. This CH−π interaction seems to be a major factor, which stabilizes the transition state of ***Z*-1A**−**C**. (2) Stabilizing dispersive interactions (stacking), which extend from the diene system to the pyrrolidine moiety (Figure 10A). (3) Due to the dimension of the electrophile, the shielding group of the catalyst may still interact with the electrophile, either sterically or electrostatically. The magnitude of the stabilization effects is thus modulated by the arrangement between the electrophile and the dienamines. Remarkably, both the transition states of ***E*/*Z*-1C** exhibit an electrostatic interaction between the *meta*-trifloromethyl group and the aromatic protons of the electrophile (Figure 10B). This has the consequence that the electrophile is rotated in the direction of the trifluoromethyl substituent. The displacement of the electrophile reduces the stacking interaction between the electrophile and the diene system, particularly in the transition state of ***E*-1C**. In total, the TS ***Z*-1C** showed better electrophile−dienamines interactions (2.7 kJ/mol) than the TS ***E*-1C**.

In contrast, in the transition state of ***E*-1A**, such electrostatic interaction between the electrophile and the shielding moiety of the dienamine does not exist, and the electrophile is not

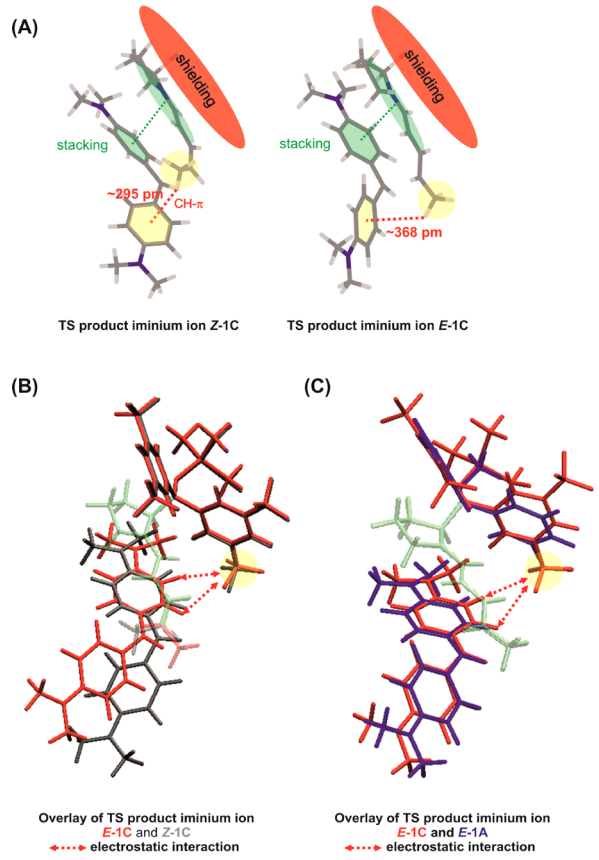

Figure 10. Transition states of iminium ion product formation and their intermolecular interactions: (A) a closer distance shows a stronger CH−π interaction in [E$^+$-***Z*-1C**]‡. (B) The alignment of the two dienamines subsystems (green) reveals the different arrangements of the electrophile; (B and C) red dashed arrows show interactions between the CF_3 group and the electrophile; (C) catalyst-dependent displacement of E$^+$-***E*-1C** compared to E$^+$-***E*-1A**.

displaced (Figure 10C). Therefore, the magnitude of the stacking interaction is considered to be equal for both ***E*/*Z*-1A**. In this case ***E*-1A** is becoming marginally more stable than ***Z*-1A** (−0.6 kJ/mol). In summary, the general preference of the conversion of *Z*-dienamines over *E*-dienamines seems to originate from stabilizing CH−π interactions in the transition state between *Z*-dienamine and electrophile. The significant differences of the ee values depending on the catalyst applied are caused by structural variations due to interactions between the aryl-substituents of the catalyst and the electrophile (Figure 11).

The main stereocontrol, being the iminium ion product formation, is in principle similar to the stereoselection mode proposed by Jørgensen et al. for Diels−Alder-type reactions.[2] Interestingly, also the barriers for the γ-functionalization with DEAD are similar. Considering the variability of potential reaction pathways depending on the experimental conditions recently also shown for enamine reactions,[44,45] also the nucleophilic addition to DEAD seems to be possible. In Diels−Alder reactions with DEAD, the transition-state barrier of the product formation is significantly lower than the barrier of the nucleophilic addition.[2] However, in the former reactions a downstream isomerization of the product is necessary.

A recent computational study of [5+2]-cycloaddition reactions using squareamide-derived bifunctional organo-catalysts with structural preorganization revealed similar

DOI: 10.1021/jacs.6b04008
J. Am. Chem. Soc. 2016, 138, 9864−9873

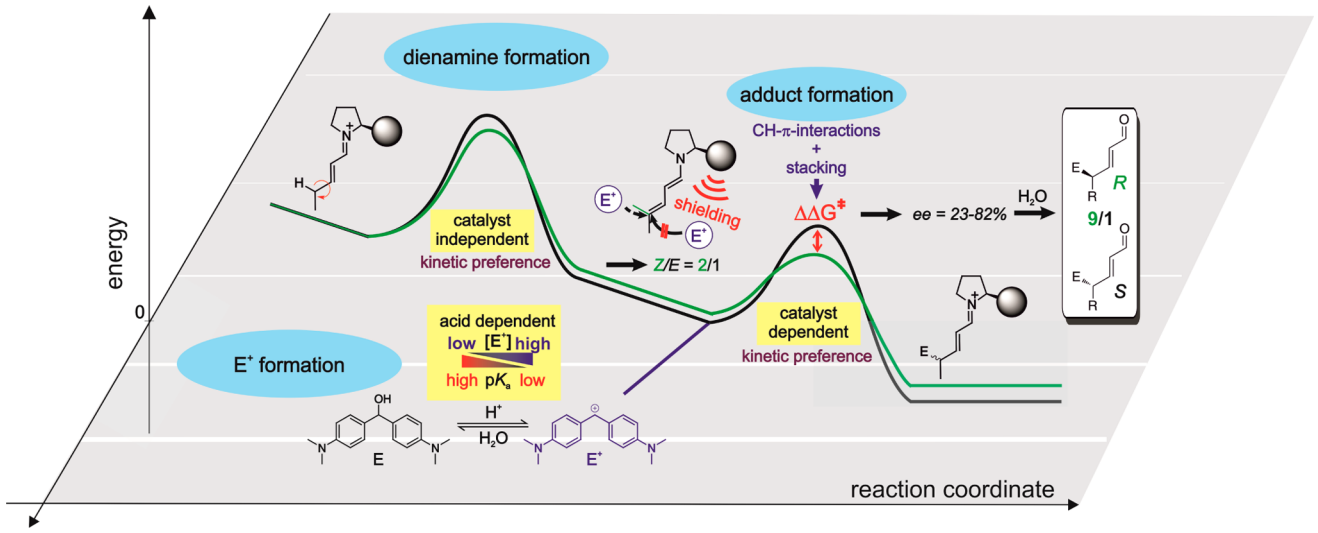

Figure 11. Schematic overview of all investigated reaction features: kinetic preference of *Z*-dienamine formation, effective shielding of the top side and catalyst-dependent reaction barriers ($\Delta\Delta G^{\ddagger}$) for electrophile-adduct formation including a kinetically controlled conversion of *Z*-dienamines and the resulting ee values.

conformational preferences (pyrrolidine puckering, *E,s-trans*) and similar noncovalent interactions (e.g., $\pi-\pi$ stacking) with respect to the formation of the stereocenter at the γ-position of dienamines.[33] Thus, independent of the system, weak dispersion interactions seem to be the key to high stereoselectivities in the dienamine catalysis. However, in our case, high stereoselectivities require additional kinetic preferences to overcome the *Z*/*E*-dilemma.

Computational Details. Geometry optimization and frequency analysis were performed with Gaussian 09 version D.01[46] at DFT level of theory using hybrid metaGGA functional M06-2X-D3/def2-SVP in the gas phase.[47−49] Subsequently, single point calculations were carried out with ORCA 3.0.3[50] at SCS-RIMP2/CBS level of theory using two points extrapolation procedure (see Supporting Information for details).[51] Solvent correction in toluene was estimated using COSMO-SAC[52−54]as implemented in CRS module of ADF2014[55−57]with COSMO potential generated by Gaussian 09 version D.01.

CONCLUSION

To summarize, for the first time, the conformational preferences of dienamine intermediates with Jørgensen−Hayashi prolinol ether catalysts were fully characterized by NMR spectroscopy. Similar to enamines, dienamines exhibit in the catalyst moiety *down*-puckering of the pyrrolidine ring and a preference for *sc-exo* conformations. For linear aldehydes, the first double bond is connected via an *s-trans* conformation and is *E* configured. For the second double bond, connected via *s-trans* conformations, the preference for *Z* configurations was confirmed. These structural studies were underpinned by theoretical calculations of the whole reaction pathway, kinetic NMR studies, and a shift of the rate-determining step by variation of the electrophile concentration. For the first time both the stereoinduction mode of dienamines in S_N-reactions and the "*Z*/*E*-dilemma of the second double bond" are explained (i.e., the missing clear correlation between the *Z*/*E* ratio and the ee values). In the case of large electrophiles, the partial shielding of the double bond by the catalyst is sufficient to effectively block attacks even in γ-position. As a result, the ee values for γ-functionalization has to correlate directly with the reaction profiles of the corresponding *Z*- and *E*-dienamines. Here, three aspects intertwine: the kinetic preference for the formation of *Z*-dienamines, the higher thermodynamic energy level of *Z*-dienamines, and the lower activation barrier for electrophile attacks from *Z*-dienamines. Theoretical studies corroborate for the first time a similar kinetic preference of *Z*-dienamine formation observed in experiments for all catalysts investigated. The main stereodiscrimination is effective in the second step, the electrophile adduct formation. Advantageous CH$-\pi$ interactions between *Z*-dienamines and the electrophile in the transition state of product iminium ion formation seem to cause faster conversions of *Z*-dienamines in general. Depending on the structure of the catalyst, different interactions between its aryl moieties and the electrophile are observed modulating the stacking between the pyrrolidine/diene and the electrophile. These structural modulations determine the level of the ee.

The secret of the highly effective remote stereocontrol in dienamines with *Z*/*E* variability of the second double bond is thus a delicate interplay of substrate, catalyst, and electrophile structure. Two factors promote high ee values: a high *Z*/*E* dienamine ratio and an effective stereodiscrimination in the product iminium ion formation. From our studies, the *Z*/*E*-ratio can be enhanced by employing short unsaturated aldehydes. Large electrophiles in combination with bulky interacting catalyst structures support an effective catalyst shielding and high stereodiscrimination for attacks from the unshielded face.

In Diels−Alder as well as S_N-type reactions, the key to high stereoselectivity in the γ-functionalization is the intermolecular interaction in the "product iminium ion transition state". In the case of DEAD as electrophile, an alternative pathway via nucleophilic addition, which is energetically comparable to S_N-type reactions, would allow γ-functionalization without downstream isomerization of the product.

DOI: 10.1021/jacs.6b04008
J. Am. Chem. Soc. 2016, 138, 9864−9873

■ ASSOCIATED CONTENT

Supporting Information

The Supporting Information is available free of charge on the ACS Publications website at DOI: 10.1021/jacs.6b04008.

Assignments of all dienamine species and products. NMR and HPLC parameters and sample preparation procedure (PDF)

■ AUTHOR INFORMATION

Corresponding Author

*ruth.gschwind@ur.de

Notes

The authors declare no competing financial interest.

■ ACKNOWLEDGMENTS

Thanks to the DFG for financial support (grant GS 13/4-1). We thank Dr. Markus Schmid for the initial NMR investigations on the structure of enamines. Many thanks to the working group of Prof. Dr. Kirsten Zeitler in Leipzig for using the HPLC.

■ REFERENCES

(1) Ramachary, D. B.; Reddy, Y. V. *Eur. J. Org. Chem.* **2012**, *2012*, 865.

(2) Bertelsen, S.; Marigo, M.; Brandes, S.; Dinér, P.; Jørgensen, K. A. *J. Am. Chem. Soc.* **2006**, *128*, 12973.

(3) Donslund, B. S.; Johansen, T. K.; Poulsen, P. H.; Halskov, K. S.; Jørgensen, K. A. *Angew. Chem., Int. Ed.* **2015**, *54*, 13860.

(4) Jia, Z.-J.; Jiang, H.; Li, J.-L.; Gschwend, B.; Li, Q.-Z.; Yin, X.; Grouleff, J.; Chen, Y.-C.; Jørgensen, K. A. *J. Am. Chem. Soc.* **2011**, *133*, 5053.

(5) Zhou, Q.-Q.; Xiao, Y.-C.; Yuan, X.; Chen, Y.-C. *Asian J. Org. Chem.* **2014**, *3*, 545.

(6) Johansen, T. K.; Gómez, C. V.; Bak, J. R.; Davis, R. L.; Jørgensen, K. A. *Chem. - Eur. J.* **2013**, *19*, 16518.

(7) Seebach, D.; Gilmour, R.; Grošelj, U.; Deniau, G.; Sparr, C.; Ebert, M.-O.; Beck, A. K.; McCusker, L. B.; Šišak, D.; Uchimaru, T. *Helv. Chim. Acta* **2010**, *93*, 603.

(8) Han, B.; Xiao, Y.-C.; He, Z.-Q.; Chen, Y.-C. *Org. Lett.* **2009**, *11*, 4660.

(9) Jurberg, I. D.; Chatterjee, I.; Tannert, R.; Melchiorre, P. *Chem. Commun.* **2013**, *49*, 4869.

(10) Marqués-López, E.; Herrera, R. P.; Marks, T.; Jacobs, W. C.; Könning, D.; de Figueiredo, R. M.; Christmann, M. *Org. Lett.* **2009**, *11*, 4116.

(11) Silvi, M.; Cassani, C.; Moran, A.; Melchiorre, P. *Helv. Chim. Acta* **2012**, *95*, 1985.

(12) Stiller, J.; Marqués-López, E.; Herrera, R. P.; Fröhlich, R.; Strohmann, C.; Christmann, M. *Org. Lett.* **2011**, *13*, 70.

(13) Talavera, G.; Reyes, E.; Vicario, J. L.; Carrillo, L. *Angew. Chem., Int. Ed.* **2012**, *51*, 4104.

(14) Jensen, K. L.; Dickmeiss, G.; Jiang, H.; Albrecht, Ł.; Jørgensen, K. A. *Acc. Chem. Res.* **2012**, *45*, 248.

(15) Marigo, M.; Wabnitz, T. C.; Fielenbach, D.; Jørgensen, K. A. *Angew. Chem., Int. Ed.* **2005**, *44*, 794.

(16) Hayashi, Y.; Gotoh, H.; Hayashi, T.; Shoji, M. *Angew. Chem., Int. Ed.* **2005**, *44*, 4212.

(17) Mukherjee, S.; Yang, J. W.; Hoffmann, S.; List, B. *Chem. Rev.* **2007**, *107*, 5471.

(18) Bächle, F.; Duschmalé, J.; Ebner, C.; Pfaltz, A.; Wennemers, H. *Angew. Chem., Int. Ed.* **2013**, *52*, 12619.

(19) Burés, J.; Armstrong, A.; Blackmond, D. G. *J. Am. Chem. Soc.* **2011**, *133*, 8822.

(20) Burés, J.; Armstrong, A.; Blackmond, D. G. *Chem. Sci.* **2012**, *3*, 1273.

(21) Duschmalé, J.; Wiest, J.; Wiesner, M.; Wennemers, H. *Chem. Sci.* **2013**, *4*, 1312.

(22) Schmid, M. B.; Zeitler, K.; Gschwind, R. M. *Angew. Chem., Int. Ed.* **2010**, *49*, 4997.

(23) Schmid, M. B.; Zeitler, K.; Gschwind, R. M. *Chem. Sci.* **2011**, *2*, 1793.

(24) Schmid, M. B.; Zeitler, K.; Gschwind, R. M. *Chem. - Eur. J.* **2012**, *18*, 3362.

(25) Schmid, M. B.; Zeitler, K.; Gschwind, R. M. *J. Am. Chem. Soc.* **2011**, *133*, 7065.

(26) Schmid, M. B.; Zeitler, K.; Gschwind, R. M. *J. Org. Chem.* **2011**, *76*, 3005.

(27) Lelais, G.; MacMillan, D. W. C. In *Enantioselective Organocatalysis*; Wiley-VCH Verlag GmbH & Co. KGaA: Weinheim, Germany, 2007; Vol. *107*, pp 95−120.

(28) Zimmer, L. E.; Sparr, C.; Gilmour, R. *Angew. Chem.* **2011**, *123*, 12062.

(29) Holland, M. C.; Metternich, J. B.; Mück-Lichtenfeld, C.; Gilmour, R. *Chem. Commun.* **2015**, *51*, 5322.

(30) Holland, M. C.; Metternich, J. B.; Daniliuc, C.; Schweizer, W. B.; Gilmour, R. *Chem. - Eur. J.* **2015**, *21*, 10031.

(31) Holland, M. C.; Paul, S.; Schweizer, W. B.; Bergander, K.; Mück-Lichtenfeld, C.; Lakhdar, S.; Mayr, H.; Gilmour, R. *Angew. Chem., Int. Ed.* **2013**, *52*, 7967.

(32) Nielsen, M.; Worgull, D.; Zweifel, T.; Gschwend, B.; Bertelsen, S.; Jørgensen, K. A. *Chem. Commun.* **2011**, *47*, 632.

(33) Roca-López, D.; Uria, U.; Reyes, E.; Carrillo, L.; Jørgensen, K. A.; Vicario, J. L.; Merino, P. *Chem. - Eur. J.* **2016**, *22*, 884.

(34) Barker, C. C.; Bridge, M. H.; Stamp, A. *J. Chem. Soc.* **1959**, 3957.

(35) Mayr, H.; Bug, T.; Gotta, M. F.; Hering, N.; Irrgang, B.; Janker, B.; Kempf, B.; Loos, R.; Ofial, A. R.; Remennikov, G.; Schimmel, H. *J. Am. Chem. Soc.* **2001**, *123*, 9500.

(36) Peelen, T. J.; Chi, Y.; Gellman, S. H. *J. Am. Chem. Soc.* **2005**, *127*, 11598.

(37) Moore, R. E.; Pettus, J. A.; Mistysyn, J. *J. Org. Chem.* **1974**, *39*, 2201.

(38) Bothner-By, A. A.; Harris, R. K. *J. Am. Chem. Soc.* **1965**, *87*, 3445.

(39) Hobgood, R. T., Jr.; Goldstein, A. J. H. *J. Mol. Spectrosc.* **1964**, *12*, 76.

(40) Cai, M.; Huang, Y.; Liu, J.; Krishnamoorthi, R. *J. Biomol. NMR* **1995**, *6*, 123.

(41) During our investigations, it was not possible to assign any α-alkylated product for our model system, because of a low signal-to-noise ratio. However, the stereoselection mode of the α-alkylation product is expected to be identical to the enamine catalysis and hence not investigated.[14] Interestingly, α,γ-doubly substituted products were detected for the first time (for assignment, see Supporting Information). The kinetic buildup of γ-alkylation products reaches a maximum followed by a decrease due to the formation of the double alkylated product. Despite best efforts (e.g., variation of acidic additive, catalyst concentration, and temperature), we were not able to influence the ratio of α- and γ-alkylation. The only variation found was an increase of doubly alkylated product by increasing the carbocation concentration.

(42) The initial increase of the *Z*/*E*-ratio (Figure 9) is most probably an artifact caused by the initially very low concentration of *E*-isomer.

(43) Note that structural analysis revealed that the most stable transition state of the product iminium ion formation exhibits an antiperiplanar arrangement (*ap*-conformation). The *exo*-conformation is marginally higher than the *ap*-conformation (∼1 kJ/mol).

(44) Ashley, M. A.; Hirschi, J. S.; Izzo, J. A.; Vetticatt, M. J. *J. Am. Chem. Soc.* **2016**, *138*, 1756.

(45) Haindl, M. H.; Hioe, J.; Gschwind, R. M. *J. Am. Chem. Soc.* **2015**, *137*, 12835.

(46) Frisch, M. J.; Trucks, G. W.; Schlegel, H. B.; Scuseria, G. E.; Robb, M. A.; Cheeseman, J. R.; Scalmani, G.; Barone, V.; Mennucci, B.; Petersson, G. A.; Nakatsuji, H.; Caricato, M.; Li, X.; Hratchian, H. P.; Izmaylov, A. F.; Bloino, J.; Zheng, G.; Sonnenberg, J. L.; Hada, M.;

DOI: 10.1021/jacs.6b04008
J. Am. Chem. Soc. 2016, 138, 9864−9873

Ehara, M.; Toyota, K.; Fukuda, R.; Hasegawa, J.; Ishida, M.; Nakajima, T.; Honda, Y.; Kitao, O.; Nakai, H.; Vreven, T.; Montgomery, J. A., Jr.; Peralta, J. E.; Ogliaro, F.; Bearpark, M.; Heyd, J. J.; Brothers, E.; Kudin, K. N.; Staroverov, V. N.; Kobayashi, R.; Normand, J.; Raghavachari, K.; Rendell, A.; Burant, J. C.; Iyengar, S. S.; Tomasi, J.; Cossi, M.; Rega, N.; Millam, J. M.; Klene, M.; Knox, J. E.; Cross, J. B.; Bakken, V.; Adamo, C.; Jaramillo, J.; Gomperts, R.; Stratmann, R. E.; Yazyev, O.; Austin, A. J.; Cammi, R.; Pomelli, C.; Ochterski, J. W.; Martin, R. L.; Morokuma, K.; Zakrzewski, V. G.; Voth, G. A.; Salvador, P.; Dannenberg, J. J.; Dapprich, S.; Daniels, A. D.; Farkas, Ö.; Foresman, J. B.; Ortiz, J. V.; Cioslowski, J.; Fox, D. J. *Gaussian 09*, version D.01; Gaussian, Inc.: Wallingford, CT, 2009.

(47) Zhao, Y.; Truhlar, D. G. *Theor. Chem. Acc.* **2008**, *120*, 215.

(48) Weigend, F.; Furche, F.; Ahlrichs, R. *J. Chem. Phys.* **2003**, *119*, 12753.

(49) Grimme, S.; Antony, J.; Ehrlich, S.; Krieg, H. *J. Chem. Phys.* **2010**, *132*, 154104.

(50) Neese, F. *Wiley Interdiscip. Rev. Comput. Mol. Sci.* **2012**, *2*, 73.

(51) Grimme, S. *J. Chem. Phys.* **2003**, *118*, 9095.

(52) Pye, C. C.; Ziegler, T.; van Lenthe, E.; Louwen, J. N. *Can. J. Chem.* **2009**, *87*, 790.

(53) Xiong, R.; Sandler, S. I.; Burnett, R. I. *Ind. Eng. Chem. Res.* **2014**, *53*, 8265.

(54) *COSMO-RS*; SCM Theoretical Chemistry, Vrije Universiteit: Amsterdam, The Netherlands, 2014; http://www.scm.com.

(55) *Amsterdam Density Functional (ADF)*; SCM Theoretical Chemistry, Vrije Universiteit, Amsterdam, The Netherlands, 2014; http://www.scm.com.

(56) Fonseca Guerra, C.; Snijders, J. G.; Te Velde, G.; Baerends, E. J. *Theor. Chem. Acc.* **1998**, *99*, 391.

(57) te Velde, G.; Bickelhaupt, F. M.; Baerends, E. J.; Fonseca Guerra, C.; van Gisbergen, S. J. a.; Snijders, J. G.; Ziegler, T. *J. Comput. Chem.* **2001**, *22*, 931.

DOI: 10.1021/jacs.6b04008
J. Am. Chem. Soc. 2016, 138, 9864−9873